Quantification of Perfusion fMRI Using a Numerical Model of Arterial Spin Labeling That Accounts for Dynamic Transit Time Effects

Luis Hernandez-Garcia,* Gregory R. Lee, Alberto L. Vazquez, Chun-Yu Yip, and Douglas C. Noll

A new approach to modeling the signal observed in arterial spin labeling (ASL) experiments during changing perfusion conditions is presented in this article. The new model uses numerical methods to extend first-order kinetic principles to include the changes in arrival time of the arterial tag that occur during neuronal activation. Estimation of the perfusion function from the ASL signal using this model is also demonstrated. The estimation algorithm uses a roughness penalty as well as prior information. The approach is demonstrated in numerical simulations and human experiments. The approach presented here is particularly suitable for fast ASL acquisition schemes, such as turbo continuous ASL (Turbo-CASL), which allows subtraction pairs to be acquired in less than 3 s but is sensitive to arrival time changes. This modeling approach can also be extended to other acquisition schemes. Magn Reson Med 54: 955–964, 2005. © 2005 Wiley-Liss, Inc.

Key words: brain; fMRI; arterial spin labeling; perfusion; blood flow

We recently presented a new two-coil approach to continuous arterial spin labeling (CASL), (dubbed Turbo-CASL) (1), that significantly enhances the temporal resolution of ASL measurements while the SNR of the measurement is maintained. An additional benefit of the technique is that its sensitivity to transit time changes can be leveraged to increase the sensitivity to brain responses. In brief, Turbo-CASL consists of a continuous labeling experiment in which the control image is collected immediately after the tagging pulse, but *before* the tag reaches the plane of interest. The tagged image is collected when the tissue concentration of the label reaches its maximum. With Turbo-CASL one can collect samples at a much faster rate compared to standard CASL techniques, and still allow for a long labeling time. In our previous publication (1) we showed that the Turbo-CASL method also had an advantage in terms of SNR per unit of time, even though the amount of accumulated tag is not allowed to reach its steady-state maximum. The method is very sensitive to transit time changes. This makes quantification of perfusion more difficult, but it can also serve to exaggerate the perfusion increases that occur during activation and hence improve detection power, as shown in our previous work. In this follow-up paper we address the quantification issues that arise as a result of these transit time changes.

Quantification of blood flow from ASL measurements is a difficult problem that requires the measurement of many parameters. A number of models have been presented to quantify perfusion, for a number of ASL acquisition schemes. These models are largely based on the first-order kinetics of the wash-in and wash-out of the inversion label into the tissue, taking into account its T_1 decay and exchange properties. The current models aim to quantify the microvascular perfusion, and consequently the larger arterial signal is routinely suppressed by the use of crusher gradients or postinversion delays. These delays have the added benefit of desensitizing the signal to the arterial transit time (ATT) (2–4). These models were developed for the cases of steady-state flow and transit time (5–10). Under such circumstances, the uptake of the arterial tag can be modeled as a linear system.

However, in addition to the flow increase, neuronal activation is also accompanied by a reduction in the ATT of approximately 10–20%, as observed by Gonzalez-At et al. (10) and Yang et al. (11). In the case of Turbo-CASL, we have calculated (1,12) that the signal can potentially change approximately 15% by a transit time change alone using the existing models.

As a result, the ASL signal observed in our Turbo-CASL approach has nonlinear characteristics that are not easily explained by existing models, and likely distort the underlying flow response. In this study we extended the general framework of the kinetics of the arterial label to the case in which flow and transit times change dynamically in a given paradigm. We then developed and implemented a method to estimate perfusion given an ASL signal from the model. We present phantom and human data demonstrating the use of the method.

THEORY

We formulated a simple numerical model for ASL based on the same principles used in the previously described analytic models (5,7). To incorporate the transit time effects, we modeled the movement and decay of the inversion tag from the tagging location to the imaging location by using the well-known transport equation in one dimension with an additional term for T_1 relaxation. Once the tag reaches the exchange location (which is the same as the imaging location), we use a first-order exchange for the uptake of the tag by the tissue compartment (5,7).

fMRI Laboratory, University of Michigan, Ann Arbor, Michigan, USA.

Department of Biomedical Engineering, University of Michigan, Ann Arbor, Michigan, USA.

Grant sponsor: Raynor Foundation; Grant sponsor: Center for Biomedical Engineering, Research and fMRI Laboratory, University of Michigan.

*Correspondence to: Luis Hernandez-Garcia, Ph.D., UM fMRI Laboratory, 2360 Bonisteel Ave., Ann Arbor, MI 48109-2108. E-mail: hernan@umich.edu

Received 14 January 2005; revised 19 April 2005; accepted 17 May 2005.

DOI 10.1002/mrm.20613

Published online 9 September 2005 in Wiley InterScience (www.interscience.wiley.com).

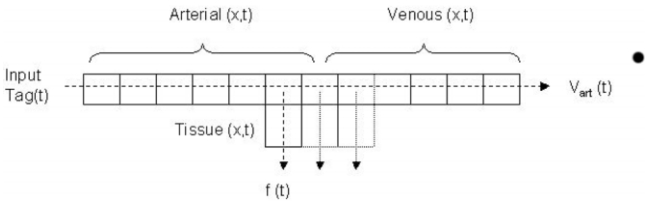

FIG. 1. Depiction of the numerical ASL model as a series of compartments. Transport and first-order exchange rate drive the movement of labeled spins into the tissue.

As depicted in Fig. 1, the model considers the arterial path from the tagging location to the exchange location as a set of discrete compartments that feed into each other. Let *A(x,t)* be the amount of tag (in units of magnetization) at position *x* and time *t*. Let us consider the longitudinal relaxation of the tag as it moves toward the exchange site. The passage of the tag through the arterial compartment, *A(x,t)*, can be characterized in general by the transport equation with a decay term that accounts for the relaxation of the label, and a second term that accounts for the exchange of the tag into the tissue (perfusion):

$$\frac{\partial A(x,t)}{\partial t} = -V_{art}(t)\cdot\frac{\partial A(x,t)}{\partial x} - R_{1art}\cdot A(x,t) - f(t)\cdot A(x,t) \quad [1]$$

where $V_{art}(t)$ is the time-varying mean arterial velocity function that reflects the observed changes in transit time along the path, R_{1art} represents the longitudinal relaxation of the tag while it is in the arteries, and $f(t)$ is the perfusion rate. Perfusion of the tag into the tissue is considered negligible ($f(t) = 0$) from the tagging plane until the exchange site, corresponding to the voxel of interest, so prior to that location we can write

$$\frac{\partial A(x,t)}{\partial t} = -V_{art}(t)\cdot\frac{\partial A(x,t)}{\partial x} - R_{1art}\cdot A(x,t) \quad [2]$$

Note that the pulsatility of the arterial flow can be built into the mean velocity function if desired, although we assume that the effect of pulsatility is negligible in this work. Let the voxel of interest be located at a distance x_d from the tagging site. At that location, the tag is partly taken up from the arteries by the tissue compartment (defined as tissue as well as microvasculature) at a variable rate *f(t)* (the perfusion function of interest).

The tissue uptake at the voxel of interest is then described by:

$$\frac{\partial T(t)}{\partial t} = f(t)\cdot A(x_d,t) - \frac{f(t)}{\lambda}\cdot T(t) - R_{1tis}\cdot T(t) \quad [3]$$

where *T(t)* is the tag content at the voxel of interest, λ is the brain–blood partition coefficient, and R_{1tis} is the longitudinal relaxation rate of the tag while it is in the tissue. It is assumed that the tag will spend enough time in the tissue to decay completely before it reaches the venous compartment, so the outflow term in Eq. [3] is neglected and the venous contribution to the signal is not considered. It must be noted that Eq. [3] is mostly the same formulation of the ASL problem at steady-state conditions proposed by others (5,7). The key difference is the input to the tissue, as we consider the ATT (and hence the mean arterial velocity) to be a time-varying function. While this is a small effect in the steady-state regime, it is very significant in the Turbo-CASL regime for functional MRI experiments.

The initial conditions of this problem are that $A(x,0) = 0$ for all x, and $T(0) = 0$. The system is driven by a tagging input function:

$$A(0,t) = M_0^{art}\cdot\alpha\cdot \mathrm{RF}(t) \quad [4]$$

in which M^o_{art} is the arterial magnetization, α is the inversion efficiency factor, and RF(*t*) is the radiofrequency pulse train used for the labeling scheme of interest. In the both CASL and Turbo-CASL, RF(*t*) is a boxcar with the appropriate duty cycle. In pulsed techniques, such as flow-sensitive alternating inversion recovery (FAIR), the system is driven by an input function that is applied every two TRs into the labeling region only:

$$A(x,t) = \alpha \text{ for } x\in[0.x], t = [2\cdot \mathrm{n}\cdot \mathrm{TR}] \quad [5]$$

In other words, every two TRs, the inversion pulse introduces a fresh tag into the slab. The rest of the time, the movement of the arterial contents is described by Eqs. [1] and [2]. In this case, x_s is equivalent to the slab width in the slice-selective case, and the to the whole system in the nonselective case. The gap between the labeling slab and the imaging slice is $x_d - x_s$.

In the presence of flow crusher gradients to spoil arterial signal, the usual ASL subtraction signal is given by *T(t)*. The nonlinearity posed by the time-varying $V_{art}(t)$ function makes finding a closed-form solution to the system quite challenging, but this formulation lends itself nicely to a numerical implementation in which the evolution of *A(x,t)* and *T(t)* are computed for all time steps using a scheme such as the Lax-Wendroff algorithm. Note that it is not possible to perform Runge-Kutta simulations, because the system includes partial derivatives.

Estimation

In practice, the parameter of interest is the flow function *f(t)* given an ASL signal, but because the instantaneous velocity function, $V_{art}(t)$, is also unknown, we need the ability to simultaneously estimate the perfusion and mean arterial velocity functions given an ASL time series. This can be done by iteratively minimizing a cost function that consists of the least-squares difference between the predicted and measured signals.

This estimation problem is challenging because it is nonlinear and underdetermined (we need to estimate two *N*-vectors, *f* and V_{art}, from a single *N*-vector of ASL measurements). There are a number of techniques we can apply to the problem to make it more manageable. Fortunately, we have prior knowledge about the unknown vectors that we can use to constrain the fitting algorithm. Such prior knowledge includes the range of values that are physiologically reasonable for perfusion and transit time under resting and activation conditions (10–14). (One could further narrow this range by measuring the baseline

perfusion of each individual subject in a standard CASL experiment.)

From previous studies (1,10,14) of transit time under rest and activation, we can clearly infer that there is a high degree of correlation between the mean arterial velocity and the perfusion vectors (a 50% increase in perfusion during activation is typically accompanied by a 10% decrease in transit time). While we do not yet know the exact relationship between the two parameters, we can make a first-order Taylor series approximation of the change in velocity from the change in perfusion, i.e., assume that the increase in mean arterial velocity from baseline is linearly related to the increase in perfusion relative to baseline, or

$$\frac{V_{art}(t) - V_{art}(0)}{V_{art}(0)} = \kappa \cdot \frac{f(t) - f(0)}{f(0)} \qquad [6]$$

where $V_{art}(0)$ and $f(0)$ refer to the resting mean velocity and perfusion (initial conditions), respectively. This assumption allows us to eliminate the $V_{art}(t)$ vector from the search space and make the problem well-determined by making a measurement of ATT during resting state only. Note that such a transit time measurement is required for Turbo-CASL techniques (1,13), and in this case it also yields the initial value of the velocity function.

In addition to constraining the search for the flow function to a physiologically plausible range (e.g., from 0 to 3 mL/s/g), we also can expect the perfusion response function to be smooth and continuous, and thus impose a roughness penalty onto the cost function in the form of a derivative of the perfusion estimate.

In summary, given this prior information and the ASL subtraction signal, $y(t)$, we can estimate the perfusion time course by searching for the function ($f(t)$) that minimizes a cost function consisting of the least-squares difference between the synthesized data and the modeled signal, plus the magnitude of the time derivative of $f(t)$ weighted by a roughness penalty factor, ρ. The perfusion estimate function is given by

$$\hat{f}(t) = \text{argmin}_{f(t)}\left\{\|y(t) - \hat{y}(t)\| + \rho\left\|\frac{d}{dt}f(t)\right\|\right\} \qquad [7]$$

This minimum can be found iteratively by a number of search algorithms, such as conjugate gradient descent, simplex, etc. As discussed below, we found the Levenberg-Marquardt algorithm to be well suited for the task.

MATERIALS AND METHODS

Simulations

To investigate the feasibility of iterative estimation approaches, we performed a set of simulations of ASL experiments during an event-related activation paradigm consisting of three activations separated by 15-s intervals over a 100-s scanning period. The simulated peak perfusion increase from a single event's response was 40% following a gamma-variate function. The mean arterial velocity was assumed to increase up to 8% from its baseline proportionately with perfusion increases. This synthetic perfusion function was sampled at TR seconds.

Table 1
Simulated ASL Acquisition and Physiological Parameters

TR	1.0 s (turbo), 3.7 s (CASL)
Tagging time	0.8 s (turbo), 3.5 s (CASL)
Tagging distance (x_d)	12 cm
Spatial sampling of path (Δx)	0.5 cm
Temporal sampling period (Δt)	1/25 s
T_{1art}	1.6 s
T_{1tis}	1.2 s
Inversion efficiency, α	0.85
Resting mean arterial velocity, $V_{art}(0)$	10 cm/s
Arterial magnetization M_{art}^0	6000
Resting perfusion, $f(0)$	0.015 ml/s/g (90 mL/min/100 g)
κ (or dV_{art}/df)	0.2

The ASL signal was simulated for both the turbo and standard CASL approaches using the acquisition parameters in Table 1 and the model described in the Theory section. Specifically, we updated the tag contents in all the space compartments (Δx) along the arterial path and the tissue compartment at finite (Δt) time intervals over the experimental period. The updates were computed following the Lax-Wendroff algorithm. To update the tag contents, the perfusion and velocity functions were upsampled to Δt. The system was modified to include the effect of the tag "destruction" that occurs during imaging by setting the amount of built-up label to zero in both the arterial and tissue compartments.

The ASL signal was calculated by downsampling the tissue function back to TR seconds, and separating the samples from every other acquisition into "tagged" and "control" time series. These two time series were sinc-interpolated and subtracted to yield the final ASL signal, as is typically done in ASL protocols (15,16). We then compared the flow to the ASL signal over time to assess the systematic errors in each approach.

Estimation: Determining an Appropriate Roughness Penalty

We estimated the perfusion function from the simulated Turbo-CASL signals under noiseless and 10% white Gaussian noise conditions. We used the Levenberg-Marquardt search algorithm, as implemented in Matlab's (The Mathworks, South Natick, MA) *lsqnonlin* function. We specified the cost function to be Eq. [7]. The upper and lower bounds allowed for the solution were 0.0075 and 0.038 mL/s/g (50% and 250% of the original guess). The maximum number of allowed iterations was set to 10 in order to limit the computation time while taking advantage of the fast convergence of the algorithm. It must be noted that the estimation algorithm could be trapped in local minima if the initial guess was far from the true mean perfusion (a difference of more than ~0.005 mL/s/g (30 mL/min/100 g)) over the function. To avoid this issue, we initially estimated the mean perfusion over the experiment as a single parameter, and used that single perfusion value as the initial guess for the estimation algorithm.

We assumed knowledge of the acquisition parameters, T_1 of arterial blood and tissue, inversion efficiency, and M_{art}^0. The initial guess consisted of a flat line of 0.015 mL

s^{-1} g^{-1} (or 90 mL/min/100 g), which was known a priori as the baseline perfusion, and is near the mean perfusion. We explored the roughness penalty by calculating bias-variance curves for values of ρ between 0 and 1000 in both the noisy and noiseless cases. The noisy case's curve was repeated 20 times, over which the bias and variance were averaged.

Estimation: Determining the Optimal Acquisition Parameters

Using the same perfusion and velocity functions, we used the model to generate an ASL signal at a range of TRs (0.6, 1.0 1.2, 1.4, 1.6, 1.8, 2.0, 2.4, 2.8, 3.2, 3.6, and 4 s). Subsequently we added a constant level of Gaussian noise to the signal, and estimated the original perfusion function from the generated signal as described. We then computed the mean squared error of the estimated perfusion function. This procedure was repeated 25 times and the errors were averaged for each TR.

Human Subjects

All human volunteers ($N = 4$) were scanned in accordance with the regulations of the University of Michigan IRB. Imaging was carried out at 3 T on a Signa LX system (GE, Milwaukee, WI, USA). ASL was accomplished by a separate transmitter coil placed on the subject's neck, as described in Ref. 17, while imaging was carried out using the standard GE birdcage coil. The labeling coil was a custom figure-8 coil (6-cm-diameter loops), which was built such that the two loops were at a 130° angle relative to each other. The labeling coil was powered by a separate signal generator (PTS 500; Programmed Test Resources Inc., Littleton, MD, USA) and RF amplifier (custom-built by Henry Radio Supply, Los Angeles, CA, USA), which was in turn gated by TTL pulses from the MRI scanner. No significant RF bleed-through or coupling between the tagging and imaging coils was found.

Resting Transit Time Measurement

Tagged-control image pairs were collected from the motor cortex using a spin-echo spiral trajectory (matrix size = 64 × 64, three slices, FOV = 22 cm, slice thickness = 7 mm, NEX = 16 pairs, TE = 17 ms, tagging pulse frequency offset = 10 KHz, tagging distance = 17–21 cm, flow crushers = b~4 s^2/mm). Our previous work (1) showed that the maximum signal in ASL is obtained when a steady state of tag accumulation is reached, and the second highest ASL signal is obtained when the tagging time approaches the transit time. Hence, in order to measure the ATT, the tag duration was varied between 600 and 2300 ms and TR was always 180 or 200 ms longer than the tagging time. These tagging time durations typically encompass the ATT from the inversion plane in the neck to the slice of interest in humans (1). The mean ATT from the tagging to the imaging location was determined by fitting the data to the model presented by Buxton et al. (5) using the approach presented in Ref. 1. An additional scan with TR = 4 s was included to improve the fit, and also to serve as a steady-state CASL measurement for reference.

Active Transit Time Measurement

The transit time during activation was measured by repeating the procedure while the subjects performed a self-paced finger opposition task. Because the steady-state CASL technique is more insensitive to transit time changes and the signal is largely proportional to perfusion, these long TR scans also served to measure the relative change in perfusion during prolonged activation.

T_1 Maps

T_1, and M_0 maps of the slices were calculated from the resting transit time data curves. By averaging only the control scans at each TR, the flow effects were eliminated, which made these data essentially the same as those obtained in a saturation-recovery experiment (i.e., the same scan repeated with a range of TRs). We estimated M_0 and T_1 by fitting the saturation recovery equation $M(\mathrm{TR}) = M_0 (1 - \exp(-\mathrm{TR}/T_1))$ at each voxel.

ASL Activation Experiments

Perfusion-weighted images were then collected during a motor cortex activation paradigm consisting of an event-related finger-tapping task (2 s tapping followed by 18 s rest, repeated 30 times). The ASL data were collected using the Turbo-CASL scheme with a TR that was approximately equal to the active transit time of each subject. This transit time was approximated as the TR that yielded maximum contrast (this is also the most negative ASL signal after the subtraction, while the longest TR yields the most positive ASL signal) in the above active transit time measurement experiment, as demonstrated in Ref. 1. The tagging time was 200 ms shorter than the TR. Note that this approach optimizes the Turbo-CASL sequence for the active case, and hence exaggerates the perfusion responses. This exaggerated response occurs because the Turbo-CASL sequence is not optimized during the resting state. However, since the transit time is reduced during the activation, the Turbo-CASL sequence becomes optimal because the transit time is roughly the same as TR during activation but not during rest.

Both control and tagged images were sinc-interpolated in time at every acquisition, effectively upsampling the time series from two to one TR. The resulting tagged-control pairs were subtracted to yield a perfusion-weighted time series of images. Active voxels were identified from the blocked design (standard CASL) data through correlation to a boxcar reference function, and time courses were extracted from the selected voxels from the activation experiments. The time courses were averaged over the selected active voxels.

Estimation of the perfusion time series in the event-related paradigm: The perfusion function was estimated from the event-related experiment's extracted time course by the numerical procedure described above using a regularization parameter of 300. Inversion efficiency was assumed to be 0.85, T_1 was averaged over gray matter, and $T_{1\mathrm{art}}$ was assumed to be 1.6 s (18). M_0^{art} was approximated from the M_0 map using the relationship $M_0^{art} = (M_0^{\mathrm{tissue}})/\lambda'$, where λ' is the blood–brain partition coefficient, adjusted for T_2 decay of both blood and tissue, as described by

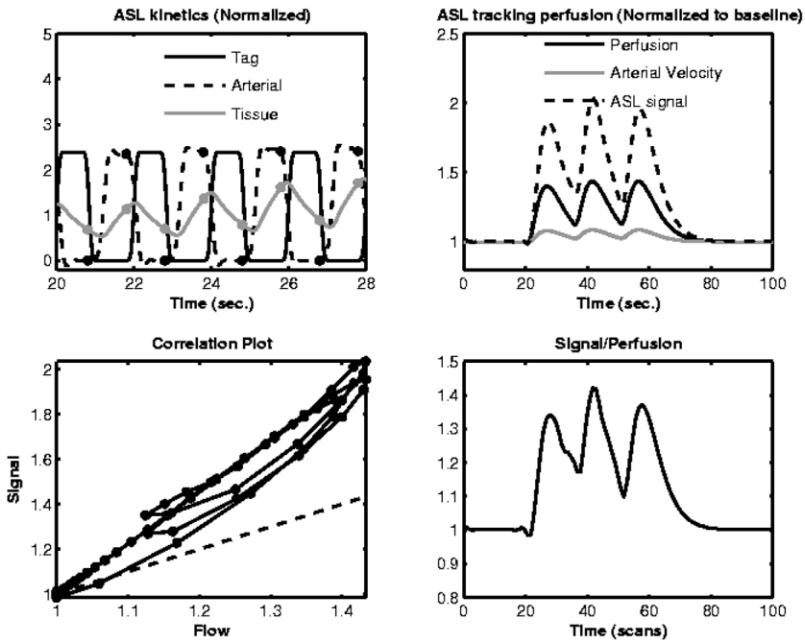

FIG. 2. Simulated Turbo-CASL time series with three "events." The top left panel shows in detail the normalized tag concentrations in the arterial and tissue compartments at the uptake (imaging) site. The concentrations are superimposed onto the labeling function over an 8-s time window. The top right panel shows the flow and velocity functions over time along with the calculated ASL signal all normalized to their baseline level. Note how in the Turbo-CASL regime, the ASL signal increase exaggerates the true flow response. The bottom left panel shows a correlation plot of the normalized ASL signal vs. the true underlying perfusion. The bottom right panel shows the same relationship as the ratio of the normalized ASL signal to the underlying flow. Note the hysteresis of the measurement.

Buxton et al. (5). The instantaneous change in velocity was assumed to be 24% of the change in perfusion during activation ($\kappa = 0.24$). This approximation is based on the estimated slope of the mean velocity and perfusion increases (see Results section). The relative perfusion change was obtained from the steady-state CASL experiment (TR = 4 s) acquired at rest and activation. Under steady-state conditions of labeling and perfusion, the ASL signal is directly proportional to perfusion. The resting mean arterial velocity was computed from the distance to the tagging plane and the ATT.

A perfusion impulse response function was calculated from the estimated perfusion function by deconvolving a comb function from the perfusion function (19,20). The comb function was created such that its value was one during the activation times, and zero otherwise.

RESULTS

Simulation

The results of our simulations can be seen in Fig. 2, for the Turbo-CASL regime, and in Fig. 3 for the standard CASL regime. The amplitude of the Turbo-CASL signal was nonlinearly related to the underlying flow function as a result of the varying transit time. For the acquisition parameters chosen, this nonlinear relationship makes the ASL signal exaggerate the true flow increases in the activation. We also observed a hysteresis in the signal caused by the lag in the amount of tag in the tissue relative to the perfusion rate (it takes a nonzero amount of time to reach the new equilibrium point when perfusion changes).

In the standard CASL experiment, we observe that the relationship between the amplitude of the signal and the flow changes is closer to linear, but the lag, and consequently the hysteresis, is more pronounced.

The estimated perfusion obtained from the Turbo-CASL simulated data can be seen in Fig. 4, which shows the perfusion estimates overlaid onto the underlying true perfusion in the noiseless and 10% noise cases at different regularization levels ($\rho = 0$, 200, 400, 600, 800, and 1000). Figure 5 shows the variance-bias plots for regularization levels of 0–1000, at 100 intervals. It is apparent from the figures that the estimation process is unstable without the regularization parameter, and produces artifactual ringing in the perfusion function estimate.

Indeed, with zero regularization, perfusion estimates from noisy simulations produced very high variance and bias (3.6e-3 and 4.0e-5). At regularization levels of $\geq$100, the variance-bias plot follows the usual pattern. In other words, as we increase the regularization parameter, the estimation is more biased toward a smoother model and the mean residual variance of the fit is also reduced. The noiseless case also behaves in an unstable pattern when the regularization is less than 200, but returns to the expected pattern above that level.

Figure 6 shows the results of the estimability tests. In this figure, the percent error in the estimation is the least when the choice of TR is within 200 ms of the resting transit time. The error also becomes smaller as the choice of TR gets closer to the steady-state continuous ASL range. The worst error occurs when the choice of TR is significantly lower than the transit time of the arterial blood. There is another local maximum of the estimation error where the ASL signal changes sign. These findings reflect the SNR properties of the ASL signal as a function of TR (1).

Human Studies

Table 2 shows the parameters obtained from the resting and activation steady-state measurements of perfusion and transit time. T_1 and M_0, obtained from the fit of the saturation recovery curve were found to be 1.24 $\pm$ 0.12 s and 3960 $\pm$ 557 (a.u.). The relative perfusion increase was

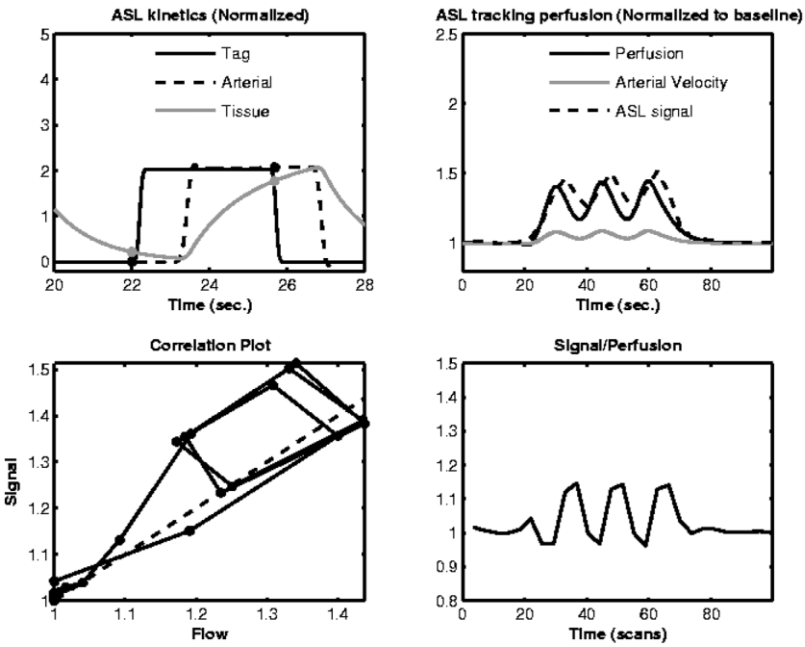

FIG. 3. Simulated CASL time series with three "events." The top left panel shows the normalized tag concentrations in the arterial and tissue compartments at the uptake (imaging) site. The concentrations are superimposed onto the labeling function. The top right panel indicates that the standard CASL method does not exaggerate the responses as much as the Turbo-CASL method, but the ASL signal lags the flow change and is sampled at a low rate. The bottom left panel shows shows a correlation plot of the normalized ASL signal vs. the true underlying perfusion. Note that the hysteresis of the measurement gets worse in the slower labeling scheme. In the bottom right panel the ratio of the normalized ASL signal to the underlying flow indicates less discrepancy in the flow increase, and the error is dominated by the delay in response detection.

obtained from the steady-state CASL measurements (TR = 4 s), since that measurement is less sensitive to dynamic transit time changes and is easily corrected when perfusion and transit time remain steady during the experiment. The transit times were reduced by 14.2% ± 12.6% during activation, which means that there was an increase in mean velocity between the tagging plane and the tissue of interest of 18.8% ± 20.2%. After correction for T_1 decay during transit time, perfusion was found to increase by 85.1% ± 61% during activation. The ratio between the change in velocity and perfusion (κ in Eq. [6]) was 0.21 ± 0.097. The same parameter was also computed through linear regression of the perfusion and velocity changes, producing a value of $\kappa = 0.24$.

The event-design experiment in the CASL regime yielded an activated region in the motor cortex, as expected. A typical activation map can be seen in Fig. 7. The time series from those voxels that were found to be active were averaged and analyzed together. The perfusion function was estimated from the whole time series using the procedure described above. The resulting time courses can be seen in Fig. 8, in which the raw ASL subtraction over the whole Turbo-CASL event-related experiment is shown in blue. The estimated perfusion function is overlaid on top of it in green. The dashed blue line represents the ASL signal that results from modeling the ASL signal given the extracted perfusion function and the measured constants. They show excellent agreement.

A perfusion impulse response function was obtained by deconvolving (18,19) the stimulation paradigm, represented by a spike train, from the perfusion time series obtained from the estimation procedure. The mean perfusion impulse response function obtained from all the subjects pooled together can be seen in Fig. 9. The resting perfusion was found to be 0.017 ± 0.0033 mL/s/g (or 102 ± 20 mL/min/100 g), and the peak perfusion was 0.022 ± 0.0024 mL/s/g (or 134 ± 14 mL/min/100 g) approximately 6 s after the onset of the activation. The rise in perfusion was followed by a long slow undershoot to approximately 12% from the baseline at 13 s. Perfusion did not completely recover until approximately 25 s after the stimulus onset.

DISCUSSION

In our previous work (1) we introduced Turbo-CASL, a rapid ASL technique that offered SNR gains over standard CASL techniques. Turbo-CASL offers an added benefit of increased sensitivity to cerebral activations because of the added sensitivity to transit time changes (14). The main drawback of the technique is that it is difficult to quantify the dynamic perfusion function from the Turbo-CASL data. In this article we present a model that addresses that issue and enables us to quantify perfusion from Turbo-CASL data. Although the motivation for developing this nonlinear model was to be able to quantify perfusion in transit-time sensitive schemes such as Turbo-ASL and Turbo-CASL (1,21), one can easily extend the numerical approach to other acquisition schemes that behave more linearly by adapting the RF input function's temporal profile and location. For example, in the case of FAIR, one could simply set the tag contents of all the arterial compartments in the tagging region (i.e., from $x = 0$ to $x = x_d$ minus the inversion gap) to be determined by the input function. Note that using this numerical approach is computationally expensive, so it may not be advantageous to do so in the slower ASL implementations that are not sensitive to transit time effects.

The perfusion responses obtained from the model estimation procedure were in good agreement with the typical perfusion values reported in the literature. Despite this agreement, however, there are a number of issues involving this technique that must be taken into consideration.

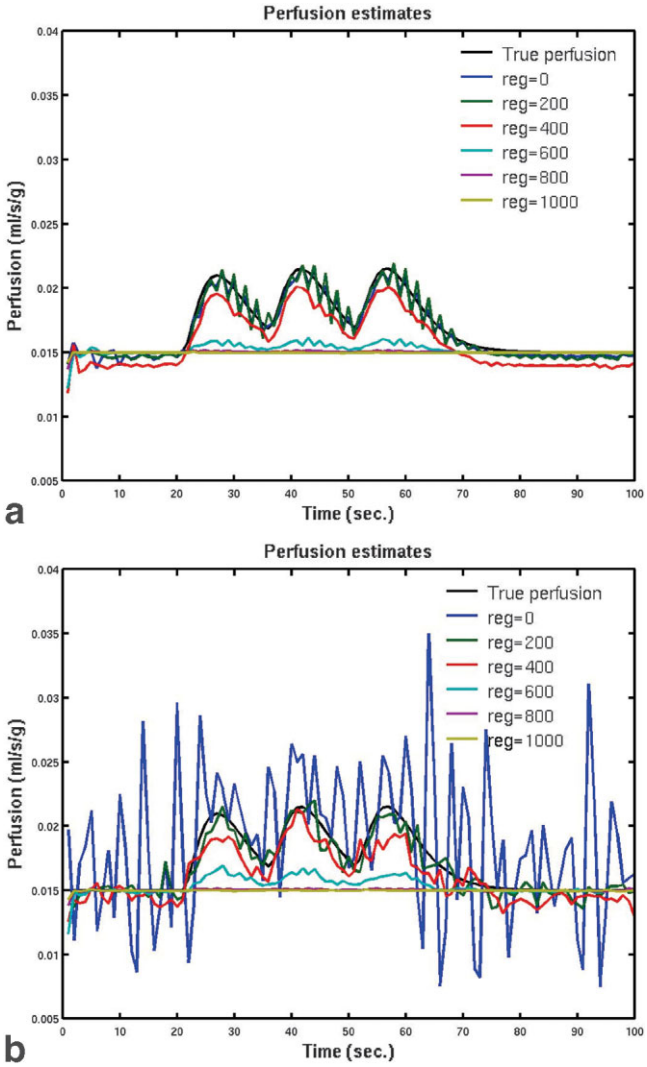

FIG. 4. **a:** ASL signal (not shown) was modeled from an arbitrary perfusion function (black). The perfusion function was then estimated from the ASL signal using different levels of regularization. In the noise-free simulations, the estimation proved to be unstable without any regularization. Including a roughness penalty proved to be very beneficial. **b:** In the noisy simulations, the roughness penalty was helpful in removing the instability, and had the beneficial effect of filtering high-frequency noise.

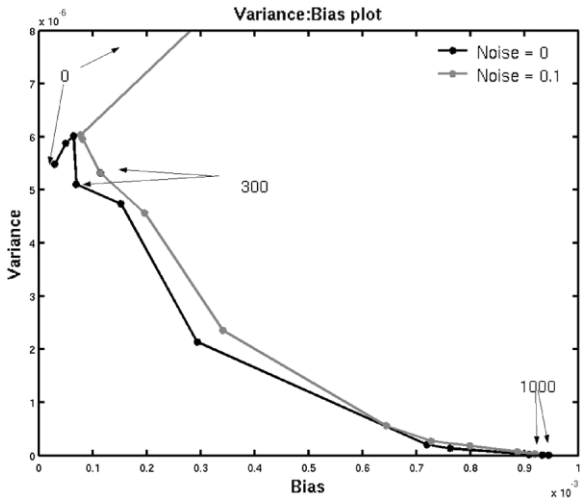

FIG. 5. Variance-bias plots for regularization levels 0–1000, at 100 intervals from noiseless and noisy simulations. As the roughness penalty is increased, the variance (caused mostly by high-frequency noise) of the estimate is reduced, but the estimate is also more biased toward a flat line. At zero regularization, the variance and bias of the noisy estimation are 3.6e-3 and 4.0e-5, respectively, which are outside the plotted range.

Since the turbo techniques are quite sensitive to changes in transit time, as we previously showed (1), it is crucial to obtain an accurate measurement of the resting ATT. Although a full error analysis of the technique is beyond the scope of this article, we noted that this parameter plays a crucial role in the measurement, and the relationship between the error in transit time and the error in the modeled signal is nonlinear. We also noted in our simulations that error in the parameter κ (increase in velocity relative to increase in perfusion) has a relatively small effect on the estimated perfusion. In our simulations, for example, a 40% increase in perfusion yields a 90% increase in ASL signal at the peak of the activation when $\kappa = 0.20$. If κ is assumed to be 0.25 (i.e., overestimated by 25%), the signal increase becomes approximately 105% (not shown). Conversely, the signal increase is 80% if κ is assumed to be 0.15 (i.e., underestimated by 25%). The baseline ASL signal is independent of κ, so it does not affect the estimation of baseline perfusion.

For the estimation data presented here, we used the value of κ measured at steady state in the activated clusters, but it may not always be feasible to make such a measurement in all clusters because many paradigms do not lend themselves to a blocked design. Hence, it may be

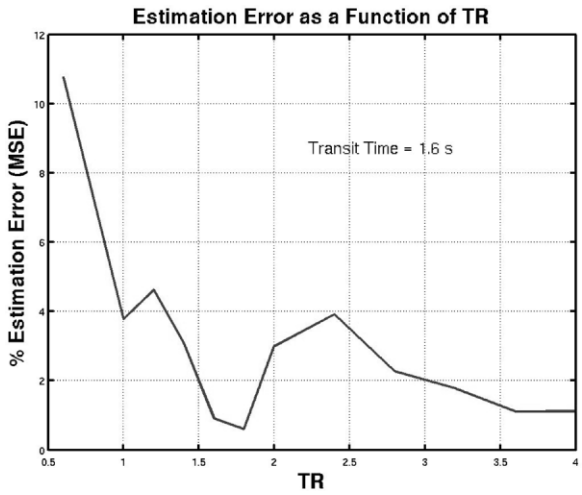

FIG. 6. Simulated estimation errors (MSEs) at different TRs given a single, known transit time. The worst error occurs at very short TRs, as well as the TR at which the ASL signal crosses over from positive to negative (2–2.5 s in this case). In both cases, there is little ASL signal.

Table 2
Measurements from SR Curves

Subject	T_1 (s)	M_0	*Ttrest* (s)	*Ttact* (s)	% $r\Delta TT$	% $r\Delta V_{art}$	% $r\Delta F$	*k*
1	1.40	3647	1.87	1.70	–9.32	10.3	37.0	0.28
2	1.16	3662	2.36	1.59	–32.8	48.9	182	0.27
3	1.30	4795	1.92	1.83	–4.72	4.96	72.0	0.069
4	1.13	3738	1.83	1.65	–9.99	11.1	49.1	0.22
Mean ± SD	1.24 ± 0.12	3960 ± 557	2.00 ± 0.25	1.69 ± 0.10	–14.2 ± 12.6	18.8 ± 20.2	85.1 ± 6	0.21 ± 0.097

more practical to make measurements of κ from visual or motor stimulations, or to use tabulated values from the literature. Using Yang et al.'s (11) human transit time data, and accounting for tagging distance in a pulsed ASL (PASL) experiment, we obtain a value of $\kappa = 0.25 \pm 0.026$ in the motor cortex. Gonzalez-At et al.'s (10) transit time and perfusion data using a CASL setup yield values of κ of 0.66 ± 0.52 and 1.2 ± 0.97 (depending on which model) in the motor cortex, and $\kappa = 3.8 \pm 3.6$ and 3.0 ± 2.2 in the visual cortex. While data from the first study yield results in agreement with our own, those from the second study do not. Gonzalez-At et al. (10) reported changes in perfusion that were much lower than ours (about a 20% change in perfusion during activation), likely because they selected a much broader ROI that was not defined by statistical tests, from the which perfusion and transit times were averaged together. We hypothesize that the discrepancy arises from the averaging of transit times and perfusion values over a broad range of values in Ref. 10, but there may be other ASL implementation issues. Having said that, it is also possible that the relationship between transit time and perfusion changes is not linear at the lower activation levels (i.e., small perfusion increases). We are currently investigating this issue in our laboratory using gradual stimulation and graded hypercapnia experiments. A potential confound of this technique is the inhomogeneity of transit times over the region of interest (ROI). In general, the strategy outlined here requires measurement of a transit time map in the resting state so that variation of transit times can then be accounted for by the model, but large variation of the transit time over the region means that the optimal Turbo-CASL acquisition parameters are not the same for the whole region. In that case, the exaggerated responses that make Turbo-CASL so appealing can be lost if the choice of timing parameters is in great disagreement with local transit times. One should note the range of TR for which perfusion can be estimated using this model for a given transit time is quite large, as demonstrated in Fig. 6. The bias in that example is less than 5% when TR is chosen to be greater than 1 s for a region in which the transit time is 1.6 s. The bias becomes quite large, however, when TR is below that value. Hence, there is an ample range for which the method can be used to estimate the perfusion function, whether the perfusion responses observed are exaggerated or dampened, as long as a transit time measurement is made.

We must also consider the dispersion of the arterial tag over the trajectory from the tagging to the imaging location because of laminar, turbulent, and pulsatile flow. It should be pointed out that the dispersion effect of the arterial tree is typically neglected in the predominant ASL models (5,7) because it is masked by the dispersion of the input function that occurs during the uptake of the tag by the tissue, and is hence a small effect. However, the dispersion effect of the arterial network can be observed in uptake curves when no flow crushers are employed (4,10). By inspecting these uptakes curves, one can approximate the dispersion either by smoothing the input function with a Gaussian kernel, or including additional higher-order derivative terms (diffusion) in the transport equation. In our simulations, which did not include any dispersion terms, we accounted for the dispersion by smoothing the input function with a Gaussian kernel of 0.25 s SD. This approximation is based on previous measurements at our laboratory (unpublished data). Although the width of the dispersion kernel has a small effect on the ASL signal, we are currently investigating in greater depth the effects of the arterial dispersion, and alternative ways to include the dispersion into the model. Hrabe and Lewis (22) recently examined dispersion effects in an analytical model of spin labeling for PASL. Their simulations modeled the dispersion as Gaussian kernel applied to the input function, given that in a PASL experiment the dispersion in the trailing edge of the tag bolus is greater than in the leading edge, since it has longer time to travel to the imaging slice. This is, in essence, the approach we have taken in our work: we convolve the input function with a Gaussian kernel. It should be noted that in our CASL experiment, the dispersion of the input function does not need to be asymmetric, as it does in the PASL experiment.

In our numerical simulation, we also included the effect of sampling the tag at the slice of interest. In practice, the accumulated tag is destroyed each TR when the different slices are excited by the RF pulses of the acquisition sequence, and the model must be revised to account for this effect. If the individual slices are sampled quickly enough ($<$50 ms), the destroyed tag will not have time to affect the adjacent slices. Thus, we need to "reset" the accumulated tag to zero every time the slice is acquired. The effect of destroying the tag at the voxel of interest proved to be negligible.

Computation time is an issue in this technique, as is usually the case for iterative techniques in imaging. To give a sense of the computation time, it took a 2.4 GHz, 512 MB RAM Pentium computer approximately 10 min to perform the necessary iterations of the model in order to estimate the perfusion function, given the ASL signal's 354 time points. It should be noted that the estimation procedure was performed using Matlab, and that the algorithm's estimate did not improve significantly after five iterations. Hence, the computation time can be significantly reduced by implementing the algorithm in C and reducing the

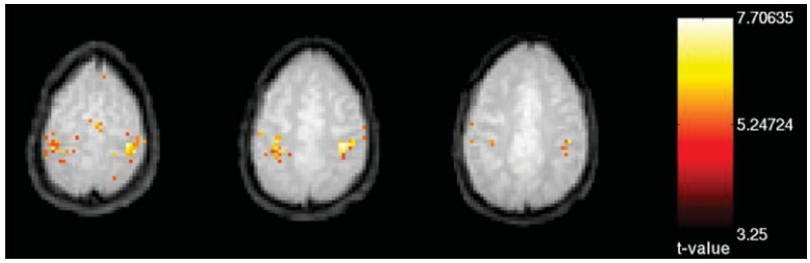

FIG. 7. Sample activation map overlaid onto anatomical images, which shows activity in the motor cortex during finger-tapping. Time courses were extracted from the active voxels to estimate the perfusion function.

number of iterations to approximately 1 or 2 min. While under our current paradigm it is not practical to estimate the perfusion function at every voxel, it is certainly practical and useful for estimating perfusion responses over an ROI. In a typical fMRI experiment, the activated regions can thus be detected through linear regression of models based on a canonical perfusion impulse response function (23), which in turn could be measured on an individual basis. Perfusion time series could then be extracted and estimated from the identified ROI only.

In terms of numerical error and stability, it is apparent that without the regularization term, the estimation problem is not stable and produces a ripple on the estimation even in the absence of noise. We believe this to be because the problem is not a well determined one (i.e., there are a large number of data points, but also a large number of unknowns in the equation). Fortunately, the addition of prior information and regularization terms alleviated the problem dramatically.

Having considered these issues, the model presented here allows us to take advantage of Turbo-ASL techniques not only to detect rapid activation events, but also to quantify perfusion given the Turbo-ASL signals. Turbo-CASL is very advantageous for event-related fMRI experiments not only because of the high temporal resolution, but because by optimizing the acquisition to the active state (shorter transit time) the perfusion responses to neuronal events appear exaggerated and are easier to detect. We find that the iterative strategy proposed in this article is very well suited for estimating perfusion from those exaggerated responses when a regularization term is included in the cost function.

Based on our experience, one can carry out a typical perfusion-based fMRI experiment by collecting a set of eight or 10 perfusion-weighted images at different TRs during the resting state. This data set yields measurements of the M_0, T_1, and ATT, and hence the optimum acquisition parameters for Turbo-CASL. The TR should be chosen to be approximately 200 ms shorter than the transit time in order to achieve the exaggerated activation effect shown here. This procedure takes approximately 10–15 min, after which the stimulation paradigm can be carried out while Turbo-CASL images are acquired. After reconstruction, motion correction, and ASL subtraction are performed, active voxels can be identified through correlation analysis (or some other method of choice), the time series can be extracted from those voxels, and the true perfusion function can be estimated through an iterative search over the model, as shown in this article.

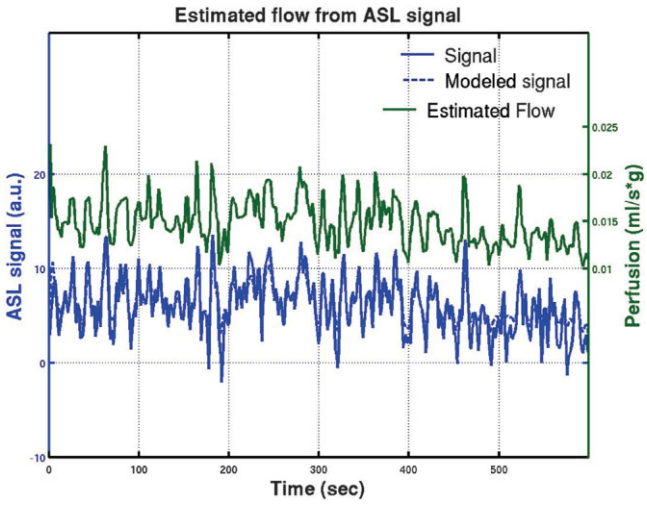

FIG. 8. Raw ASL signal extracted from the selected pixels (blue solid). From this function we estimate the perfusion function (green solid). This estimated perfusion was used to simulate the original signal (dashed blue), giving a sense of the error in the estimate.

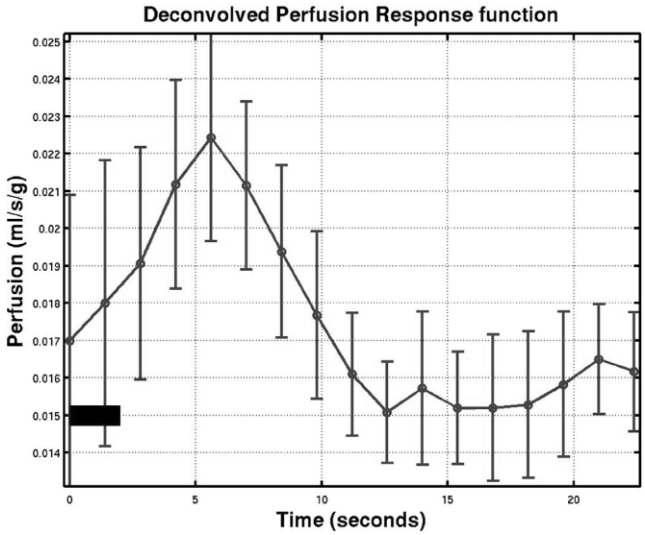

FIG. 9. Perfusion impulse response function obtained by deconvolution of the stimulus function from the ASL signal. The stimulation period is depicted by the thick, horizontal black bar.

ACKNOWLEDGMENTS

We thank Valur Olafsson for his valuable assistance.

REFERENCES

1. Hernandez-Garcia L, Lee GR, Vazquez AL, Noll DC. Fast, pseudo-continuous arterial spin labeling for functional imaging using a two-coil system. Magn Reson Med 2004;51:577–585.
2. Ye FQ, Mattay VS, Frank JA, Weinberger DR, McLaughlin AC. Comparison of white and grey matter arterial transit times in spin tagging experiments. In: Proceedings of the 7th Annual Meeting of ISMRM, Philadelphia, 1999. p 1847.
3. Ye FQ, Mattay VS, Jezzard P, Frank JA, Weinberger DR, McLaughlin AC. Correction for vascular artifacts in cerebral blood flow values measured by using arterial spin tagging techniques. Magn Reson Med 1997;37:226–235.
4. Alsop DC, Detre JA. Reduced transit-time sensitivity in noninvasive magnetic resonance imaging of human cerebral blood flow. J Cereb Blood Flow Metab 1996;16:1236–1249.
5. Buxton RB, Frank LR, Wong EC. A general kinetic model for quantitative perfusion imaging with arterial spin labeling. Magn Reson Med 1998;40:383–396.
6. Yang Y, Frank JA, Hou L, Ye FQ, MacLaughlin AC, Duyn JH. Multislice imaging of quantitative cerebral perfusion with pulsed arterial spin labeling. Magn Reson Med 1998;39:825.
7. Williams DS, Detre JA, Leigh JS, Koretsky AP. Magnetic resonance imaging of perfusion using spin inversion of arterial water. Proc Natl Acad Sci USA 1992;89:212–216.
8. Kim SG. Quantification of relative cerebral blood flow change by flow sensitive alternating inversion recovery (FAIR) technique: application to functional mapping. Magn Reson Med 1995;34:293–301.
9. Detre JA, Leigh JS, Williams DS, Koretsky AP. Perfusion imaging. Magn Reson Med 1992;23:37–45.
10. Gonzalez-At JB, Alsop DC, Detre JA. Cerebral perfusion and arterial transit time changes during task activation determined with continuous arterial spin labeling. Magn Reson Med 2000;43:739–746.
11. Yang Y, Engelien W, Xu S, Gu Hong, Silbersweig DA, Stern E. Transit time, trailing time, and cerebral blood flow during brain activation: measurement using multislice, pulsed spin-labeling perfusion imaging. Magn Reson Med 2000;44:680–685.
12. Lee GR, Hernandez-Garcia L, Vazquez A, Noll D. A fast perfusion measurement for functional imaging using double-coil AST. In: Proceedings of the 11th Annual Meeting of ISMRM, Toronto, Canada, 2003. p 739.
13. Ye FQ, Berman KF, Ellmore T, Esposito G, van Horn JD, Yang Y, Duyn J, Smith AM, Frank JA, Weinberger DR, McLaughlin AC. H(2)(15)O PET validation of steady-state arterial spin tagging cerebral blood flow measurements in humans. Magn Reson Med 2000;44:450–456.
14. Lee GR, Hernandez-Garcia L, Vazquez AL, Noll DC. Effects of activation induced transit time changes on functional Turbo ASL imaging. In: Proceedings of the 12th Annual Meeting of ISMRM, Kyoto, Japan, 2004. 519.
15. Liu TT, Wong EC, Frank LR, Buxton RB. Analysis and design of perfusion-based event-related fMRI experiments. Neuroimage 2002;16:269–282.
16. Aguirre GK, Detre JA, Zarahn E, Alsop DC. Experimental design and the relative sensitivity of BOLD and perfusion fMRI. Neuroimage 2002;15:488–500.
17. Zhang W, Silva AC, Williams DS, Koretsky AP. NMR measurement of perfusion using arterial spin labeling without saturation of macromolecular spins. Magn Reson Med 1995;33:370–376.
18. Lu H, Clingman C, Golay X, van Zijl P. What is the longitudinal relaxation time (T1) of blood at 3.0 Tesla? In: Proceedings of the 11th Annual Meeting of ISMRM, Toronto, Canada, 2003. p 669.
19. Burock MA, Dale AM. Estimation and detection of event-related fMRI signals with temporally correlated noise: a statistically efficient and unbiased approach. Hum Brain Mapp 2000;11:249–260.
20. Hinrichs H, Scholz M, Tempalmann C, Woldorff MG, Dale AM, Heinze HJ. Deconvolution of event-related fMRI responses in fast-rate experimental designs: tracking amplitude variations. J Cogn Neurosci 2000;12:76–79.
21. Wong EC, Luh WM, Liu TT. Turbo ASL: arterial spin labeling with higher SNR and temporal resolution. Magn Reson Med 2000;44:511–515.
22. Hrabe J, Lewis DP. Two analytical solutions for a model of pulsed arterial spin labeling with randomized blood arrival times. J Magn Reson 2004;167:49–55.
23. Friston KJ, Holmes AP, Poline JB, Grasby PJ, Williams SCR, Frackowiak RSJ, Turner R. Analysis of fMRI time series revisited. Neuroimage 1995;2:45–53.